INTERNATIONAL JOURNAL OF INTEGRATED ENGINEERING
ISSN: 2229-838X e-ISSN: 2600-7916

IJIE

Vol. 17 No. 8 (2025) 100-114
https://publisher.uthm.edu.my/ojs/index.php/ijie

Kinetic Study of the Hydrophobic Modified-ZnO Kapok Using Pseudo First Order and Pseudo Second Order Model for Cooking Oil Adsorption

M. A. Bukhori Hamidon[1,5], Rosniza Hussin[2,3]*, Zawati Harun[2,4], Muhamad Zaini Yunos[2,3], Ainun Rahmahwati Ainuddin@Nordin[2,3], Clement Pakiam[5], M. K. Azuan[5], U. S. Nabilah[6]

[1] *Department of Mechanical Engineering Technology, Faculty of Engineering Technology, Universiti Tun Hussein Onn Malaysia, Pagoh Higher Education Hub, Muar, 84600, MALAYSIA*
[2] *Faculty of Mechanical and Manufacturing Engineering, Universiti Tun Hussein Onn Malaysia, Parit Raja, 86400, MALAYSIA*
[3] *Nano Structure and Surface Modification (NanoSurf), Faculty of Mechanical and Manufacturing Engineering, Universiti Tun Hussein Onn Malaysia, 86400, MALAYSIA*
[4] *Integrated Material and Process, Advanced Manufacturing & Materials Centre, Faculty of Mechanical and Manufacturing Engineering, Universiti Tun Hussein Onn Malaysia, Parit Raja, 86400, MALAYSIA*
[5] *Eko Metal Industries, Juru, Bukit Mertajam, Pulau Pinang, 14000, MALAYSIA*
[6] *Faculty of Modern Language and Communication, Universiti Putra Malaysia, UPM Serdang, Selangor Darul Ehsan, 43400, MALAYSIA*

*Corresponding Author: rosniza@uthm.edu.my
DOI: https://doi.org/10.30880/ijie.2025.17.08.010

Article Info

Received: 1 April 2025
Accepted: 25 November 2025
Available online: 31 December 2025

Keywords

Kapok, kinetic study, ZnO NPs, cooking oil, adsorption

Abstract

This study investigates the kinetic behaviour of hydrophobic modified-ZnO kapok fibers for the adsorption of used cooking oil. The modification of natural kapok fibers with ZnO nanoparticles was achieved using a hydrothermal process, enhancing their hydrophobic and oleophilic properties. The adsorption kinetics were evaluated using pseudo-first-order (PFO) and pseudo-second-order (PSO) models to describe the oil sorption behaviour of raw kapok fibers (RKF) and modified kapok fibers (MKF). The study revealed that MKF (114.7 g/g) exhibited higher oil adsorption capacity than RKF (88.6 g/g) after 30 minutes adsorption period, with the PSO model providing a better fit for the experimental data by showing R^2 value close to 1 for both RKF (R^2 = 0.9942) and MKF (R^2 = 0.9781) sample. The results suggest that the modification of kapok fibers with ZnO significantly improves their oil adsorption capacity, making them a viable and eco-friendly alternative for oil spill remediation.

1. Introduction

The growing concern over environmental pollution, particularly in aquatic ecosystems, has intensified the need for efficient methods of oil spill cleanup. Improper disposal of cooking oil for example, it can lead to substantial environmental degradation, affecting water, soil, and marine life [1]. It is estimated that a single liter of cooking oil can contaminate up to 20,000 liters of water which equivalent to an individual's water consumption over 14 years [2]. Various approaches to mitigate oil pollution include in-situ combustion, which involves burning the oil

in place [3]; bioremediation, where microorganisms break down contaminants [4]; and the use of absorbing materials that capture and remove oil from water [5].

Among absorbent materials, natural fibers with unique wettability properties, such as hydrophobic-oleophilic characteristics, have shown promise in effectively separating oil from water [6]-[9]. One such material, kapok fiber, has demonstrated a high oil adsorption capacity due to its thin cell walls, large lumen, low density, and natural hydrophobic-oleophilic surface, making it an eco-friendly and cost-effective option for oil spill remediation [10]-[13]. However, the inherent smoothness of kapok fibers, caused by a waxy coating, can reduce their oil adsorption efficiency [14].

To address this limitation, this study proposes modifying kapok fiber with ZnO nanoparticles via a hydrothermal process, creating a rougher surface that enhances its hydrophobic and oleophilic properties. This modification aims to increase the fiber's oil adsorption selectivity and retention capacity, thereby improving its effectiveness in treating oily water. The study will also evaluate the sorption kinetics of the hydrophobic modified-ZnO kapok in cooking oil, contributing to the development of more efficient and sustainable methods for oil spill cleanup.

1.1 Sorption Kinetics with Pseudo-First-Order (PFO) and Second-Order Models (PSO)

Adsorption is the most frequently used method to remove contaminants from polluted aqueous media. It is also one of the most effective approaches. It is preferred over other ways due to its uncomplicated design, which makes it simple to operate and low cost and high energy efficiency [15]. The kinetic isotherm, produced empirically by recording the adsorbed amount against time, is the foundation for kinetics research. Kinetic studies create a model that describes the adsorption rate [16].

Many studies on adsorption for water and wastewater treatment have been conducted in the scientific community, focusing on either equilibrium or kinetic studies. Pseudo-first and pseudo-second-order rate laws are often used to model adsorption kinetics [17]. In a theoretical analysis by Saeid [18], the general equation translates to a pseudo-first-order model at high starting concentrations of solute (sorbate) while a pseudo-second-order model at lower starting concentrations of solute.

In other words, at high beginning solute concentrations, the sorption process follows pseudo-first-order kinetics, but at lower initial solute concentrations, it follows pseudo-second-order kinetics. The adsorption kinetics reflect the evolution of the adsorption process versus time. To explain the adsorption kinetics in group adsorption frameworks, various models portraying solute dispersion at the surface and in the pores of the adsorbent have been set up, for example, film dissemination model, intra-specific dissemination model, extra-specific dissemination model, pore dissemination model, and others.

PFO and PSO models, on the other hand, are frequently employed to characterize the adsorption rate in liquid-solid interactions [19]. Factors such as pH, starting dye concentration, adsorbent dosage, contact time, and temperature effect the kinetic studies [20]. Kinetic adsorption experiments were conducted to determine the effect of time on the adsorption process. The kinetics curves were described using linear and nonlinear models [19].

1.1.1 Pseudo First-Order Model

Jean-Pierre [21] stated that Pseudo-first order rate law, k_1. The condition for pseudo-first request energy was presented at first by Lagergren, and it is utilized in the structure proposed by Yuh-Shan and Gordon [22];

$$\ln[q_e - q(t)] = \ln q_e - k_1 t \tag{1}$$

With q and q_e is the amount of adsorbed solute and value at equilibrium, k_1 is the pseudo-first-order rate constant, and t is the time. This equation may also be written as,

$$q(t) = q_e[1 - \exp(-k_1 t)] \tag{2}$$

If q_e is determined from the experiment, the fractional uptake (with respect to equilibrium),

$$F(t) = \frac{q(t)}{q_e} \tag{3}$$

May be computed. Then one would have in the case of k_1,

$$F(t) = 1 - \exp(-k_1 t) \tag{4}$$

Int. Journal of Integrated Engineering Vol. 17 No. 8 (2025) p. 100-114

1.1.2 Pseudo-Second-Order Model

Jean-Pierre [21] also stated that Pseudo-second order rate law, k_2 the formula for pseudo-second-order energy, is utilized in the structure proposed by Ho and McKay as equation below [22]:

$$\frac{t}{q(t)} = \frac{t}{q_e} + \frac{1}{k_2 q_e^2} \tag{5}$$

which k_2 is the pseudo-second-order kinetic rate constant. Eq. (5) can also be written as,

$$q(t) = \frac{(q_e)^2 k_2^* t}{1+(q_e)k_2^* t} \tag{6}$$

with $k_2^* \equiv k_2 q_e$, or

$$F(t) = \frac{k_2^* t}{1+k_2^* t} \tag{7}$$

1.1.3 Significant of the Research

This research presents an innovative method by integrating ZnO nanoparticles into natural kapok fiber, significantly boosting its oil adsorption capabilities. The development of this cost-efficient, natural sorbent with enhanced effectiveness could decrease the dependence on costly synthetic alternatives, making large-scale oil spill remediation more affordable. The findings help advance sustainable cleanup technologies by improving the oil adsorption capacity and selectivity of this eco-friendly material.

2. Methodology

2.1 Material and Reagents

Kapok fibers have been the primary material in this research. These fibers were sourced from Mutiara Zulfikar Sdn. Bhd., a reputable supplier located in Kulim, Kedah as in Fig. 1(a). The kapok fibers procured from this supplier had already undergone processing to separate them from their seeds. This pre-processing step is crucial as it ensures that the fibers are clean, free from seed residues, and ready for immediate use in subsequent experimental procedures. The removal of seeds from the kapok fibers facilitates their application in various research and industrial processes, maintaining the integrity and quality of the fibers for accurate and reliable experimental results.

The oils used for the adsorption test was used cooking oil, UCO which was collected from Barracuda Cafe at the UTHM Pagoh residential college. Fig. 1(b) shows ZnO NPs brand: Sigma Aldrich (<100nm particle size) in dispersion form with 1.7 g/mL ± 0.1 g/mL at 25 °C, concentration 20 wt.% in H_2O and a pH of 7.5 ± 1.5 was used as a coating on the kapok fiber surface.

(a) **(b)**

Fig. 1 *(a) Processed kapok fiber from supplier; (b) ZnO Nanoparticles brand: Sigma Aldrich*

2.2 Kapok Fiber Modification

Initially, a 15 ml of ZnO NPs (particle size <100 nm) in dispersion form with a density of 1.7 g/mL ± 0.1 g/mL at 25 °C and a concentration of 20 wt.% in H_2O with a pH of 7.5 ± 1.5 was prepared using a measuring cylinder. The raw kapok fiber was cleaned and weighted to 1.0 ± 0.01 gram per sample. Fig. 2 show the raw kapok fiber modification flow.

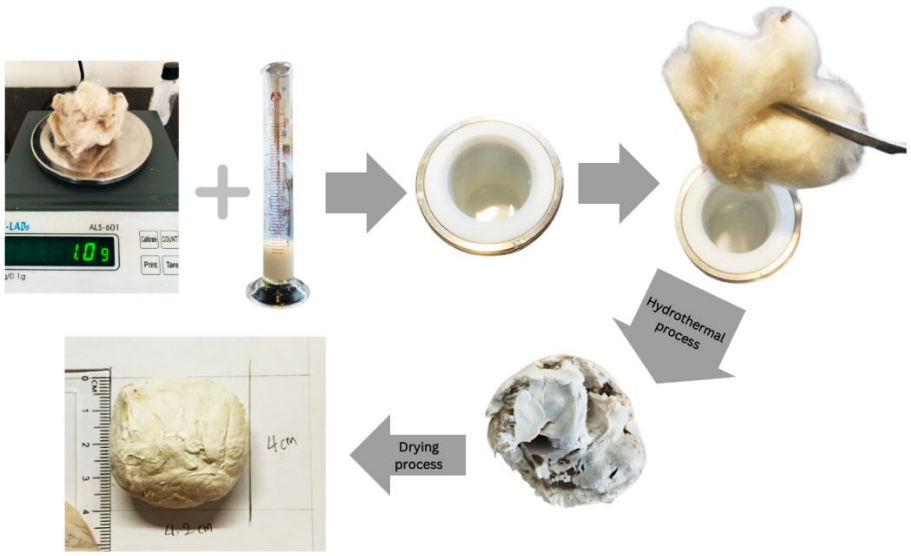

Fig. 2 *Kapok fiber modification flow*

Then, a clean raw kapok fiber was dipped inside the 15 ml ZnO NPs dispersion in steel autoclave, designed to withstand high pressure and temperature conditions. The fiber was dipped inside the ZnO NPs dispersion, ensuring full saturation. Following immersion, the autoclave is sealed to maintain the necessary high-pressure environment for the reaction. The sealed autoclave undergoes hydrothermal treatment, involved heating at 100°C for 6-hour duration, facilitating the deposition of ZnO nanoparticles onto the raw kapok fibers. After completing the hydrothermal treatment, the autoclave is cooled to room temperature before the modified kapok fiber was extracted and oven dried at 50°C for 24 hours to ensure the ZnO NPs was properly coated on the kapok fiber surface. The weight of ZnO was calculated based on Eq. (8).

$$Weight\ of\ ZnO = \frac{20}{100} \times Weight\ of\ ZnO\ dispersion\ (g) \tag{8}$$

2.3 Characterization of Raw and Modified Kapok Fiber with ZnO Nanoparticles

2.3.1 Procedure for Fourier-Transform Infrared Spectroscopy (FTIR) Analysis

The infrared spectrum of raw and modified kapok was analyzed using Fourier Transform Infrared Spectroscopy, FTIR (Agilent Technologies, USA), at the analytical laboratory in UTHM Pagoh. The spectrum was interpreted to identify functional groups or chemical bonds by analyzing the peaks, where each peak corresponded to a specific vibration between atoms in the molecules of sample. For the sample measurement, kapok fibers were cut into a small piece and placed onto the ATR crystal, ensuring uniform coverage of the crystal surface. The pressure clamp is utilized to ensure good contact between the kapok fibers and the ATR crystal. The parameters for the FTIR analysis are set as follows: two different scans were carried out at 4000 cm^{-1} to 650 cm^{-1} wavelengths, at a resolution of 8 cm^{-1} for raw and modified kapok fiber samples.

2.3.2 Procedure for Scanning Electron Microscopy (SEM) Analysis

Scanning Electron Microscopy (SEM) (EM30AX, Plus, COXEM, Italy) was operated to investigate the morphology of the kapok. This analysis was performed at the Nanotechnology Physics Laboratory in UTHM Pagoh. The kapok fibers were cut into small pieces and attached to rectangular stainless steel sample holders using conductive double-sided sticky tape. Then, the sample was cleaned using a blower to clear any visible contaminant on the surface. Initially, the kapok fiber samples underwent a pre-processing step to enhance their conductivity and imaging quality under SEM. This involved coating the fibers with a thin layer of gold (Au) using a rotary pumped coater, specifically the (Quorum Q150R S, UK) model.

The kapok fibers were carefully placed in the coater chamber, and the process parameters were set to achieve a uniform gold coating, typically around 10-20 nm in thickness. The coating process involved creating a vacuum within the chamber to facilitate the deposition of gold onto the fiber surfaces. Once the gold coating was completed, the samples were then transferred to the SEM chamber, where the SEM analysis was conducted. The SEM was operated under high-vacuum conditions, with an accelerating voltage of 20 kV, the surface morphologies of the kapok sample were recorded at magnification of x500 and x1000 providing clear images of the sample surfaces.

2.3.3 Procedure for Contact Angle Analysis

To investigate the interactions of wetting a solid by a liquid, the contact angle analysis was done using a contact angle machine (VCA Optima) at Mint-SRC in UTHM main campus (Batu Pahat). Before the contact angle analysis, kapok fibers were cut into small, manageable pieces around 1 cm length and been compressed using film glass for a week before testing date to get a flat surface. The prepared kapok fiber samples were carefully mounted on the sample stage. Only before testing, the kapok fiber was uncompressed to ensure they remained flat and stable during the measurement process. To achieve the consistent and accurate measurements, carefully avoided overlapping fibers and ensured that the surface remained as smooth and uniform as possible.

Using an automated syringe dispenser, a droplet of deionized water was carefully deposited onto the surface of the kapok fiber. The deposition was performed gently to prevent any disturbances to the droplet shape. Immediately after the droplet was placed on the fiber surface, the high-resolution camera captured images of the droplet from a lateral view. The software (AutoFast Imaging Software) then analyzed these images to determine the contact angle.

2.4 Kinetic Study on Oil Sorption

The pure oil sorption of RKF and MKF-15-6H was carried out based on research by Aimee et al. [23]. In a 200 mL beaker as a test cell, 0.1 g of kapok sample was immersed in 150 mL of used cooking oil. The kapok fibers were collected at specific intervals (10s - 30min), drained for 30s without squeezing, and weighed. The technique was repeated until equilibrium or maximal sorption capacity was achieved. The sorption capacities at each time interval (q_t) were determined using Eq. (9).

$$q_t = \frac{m_f - m_i}{m_i} \tag{9}$$

where m_f is the weight of the oil-filled fiber, and m_i is the weight of the dry fiber.

Based on previous research suggested that the time is taken for kapok fiber to reach equilibrium in cooking oil testing usually below 30 minutes which is 15 minutes, as reported by Jintao et al. [24] while Baldin et al. [25] stated that kapok fiber achieves equilibrium in cooking oil sorption within just 5 minutes of contact. However, the time to reach saturation may vary due to the differences in experimental conditions. Thus, the experiment was done for only 30 minutes.

This test determined oil sorption behaviour using the pseudo-first-order and pseudo-second-order models. The linear and nonlinear equations of the kinetic models used to fit the experimental results from the sorption of used cooking oil by raw kapok fiber (RKF) and modified kapok fiber (MKF-15-6H). Model fitting, and parameter calculations were conducted in OriginPro. The correlation coefficient (R^2) was used to assess the adequacy of the linear and nonlinear models fitted to the system.

3. Results

3.1 Modification of Kapok Fiber

Following the process outlined in subchapter 2.2, kapok fiber was modified by a hydrothermal process using ZnO NPs which shows the modification process of kapok. The coating was fragile after the hydrothermal process, as it could be easily removed from the fiber surface by weak abrasion. As a result, the sample was oven-dried to ensure that the ZnO coating was completely dried.

3.1.1 Percentage of ZnO on the Kapok Fiber Surface

The percentage of ZnO on kapok fiber was calculated to find the efficiency of this modification method, and the loss percentage of ZnO was calculated. The percentage of ZnO in 15 mL ZnO dispersion was calculated based on the information on the chemical label, which mentions that the ZnO concentration is 20 wt.% in H_2O. From this information, the 15 mL ZnO NPs in dispersion form was weighed before hydrothermal, after hydrothermal, and after drying. The initial weight of ZnO was calculated based on Eq. (8). The data for the calculation is shown in the

Table 1 below. The weight of ZnO after hydrothermal and after drying must be subtracted from the weight of kapok (1 gram) to obtain the weight of ZnO dispersion only.

The experimental data from sample MKF-15-6H provides insight into the interaction between the kapok fiber and ZnO dispersion through the hydrothermal process. The sample began with 1 gram of kapok fiber and 16.0 gram (15 mL) of ZnO dispersion, which contained 3.2 gram of ZnO. After the hydrothermal treatment, the combined weight of the ZnO dispersion and kapok fiber was 9.9 gram, while the ZnO dispersion alone weighed 8.9 gram. Only 1.78 gram of ZnO was deposited on fiber surface. This indicates that the kapok fiber successfully absorbed a portion of the ZnO dispersion during the process.

However, after drying, the ZnO retained on the kapok fiber was reduced to 0.46 gram. The difference between the initial ZnO content (3.2 gram) and the final ZnO weight (0.46 gram) suggests that a significant amount of ZnO was either not deposited onto the kapok fiber or was lost during the drying process, potentially due to unsuccessful binding or detachment of the ZnO onto fiber surface during drying. These findings suggest that while some ZnO was successfully deposited onto the kapok fiber, the process efficiency may need improvement to enhance ZnO retention. This could involve optimizing the concentration of the ZnO dispersion, the duration, and temperature of the hydrothermal treatment, or exploring additional surface treatments to increase the adhesion of ZnO to the kapok fiber. Improving these factors would be crucial to maximizing the ZnO coating on the kapok fiber for applications like oil adsorption or filtration.

Table 1 *Weight of ZnO on Kapok surface*

Sample	Weight of kapok fiber (g)	Initial weight of ZnO Dispersion (g)	Initial weight of ZnO	Weight after hydrothermal (g)			Weight after dry (g)		
				ZnO dispersion + kapok	ZnO dispersion only	ZnO	ZnO dispersion + kapok	ZnO dispersion only	ZnO
MKF-15-6H	1	16.0	3.2	9.9	8.9	1.78	3.3	2.3	0.46

3.2 Characterization Analysis for Raw Kapok Fiber (RKF) and Modified Kapok Fiber (MKF)

To comprehensively characterize raw kapok fiber (RKF) and modified kapok fiber (MKF), a combination of FTIR for chemical analysis, SEM for morphological studies, and contact angle measurements for surface properties is essential. FTIR analysis provides insights into the chemical composition and functional groups present in the fibers. SEM imaging allows visualization of the fiber surface morphology and structure, while contact angle measurements assess the wettability of the fibers.

3.2.1 Chemical Structure and Functional Group Analysis using FTIR

The functional group and chemical structure analyses for raw (RKF) and modified kapok fiber (MKF) were done using FTIR to confirm the presence of ZnO nanoparticles as in Fig. 3. The first peak, observed at 3317 cm^{-1}, is usually due to O-H stretching vibrations. The O-H stretching vibration peak at 3317 cm^{-1} is typically broad and indicates the presence of hydroxyl groups of cellulose [26]. The modified sample MKF-15-6H showed a decrease in intensity at this peak compared to RKF samples. This suggested that a successful formation of ZnO NPs on fiber surface [27]. Another peak was observed at wavenumber 2892 cm^{-1} due to C-H stretching vibrations. This peak corresponds to C-H stretching vibrations in methyl and methylene groups, common in [28]. A study by Graecia et al. [27], also stated that a peak was observed around 2929-2850 cm^{-1} wavenumber due to asymmetric and symmetric C-H stretching in CH_2 and CH_3.

The peak at 1729 cm^{-1} is associated with carbonyl groups (C=O stretching), which could derive from acetyl or uronic ester groups in hemicellulose or ester linkages in pectins [29]. Similarly, a study by Graecia et al. [27] found that a peak around the wavenumber 1741 cm^{-1} was due to C=O stretching of ketones, carboxylic, and ester groups in lignin. A peak at wavenumber 1244 cm^{-1} was observed due to C-H and C-O bending vibrations [25]. This region indicates the presence of lignin and hemicellulose, respectively, as stated by Leonard and Martin [30]. The MKF-15-6H samples displayed a minor increase in peak transmittance, which suggested a slight modification to the lignin and hemicellulose. However, the modifications did not drastically change the spectra compared to the RKF [31].

Int. Journal of Integrated Engineering Vol. 17 No. 8 (2025) p. 100-114

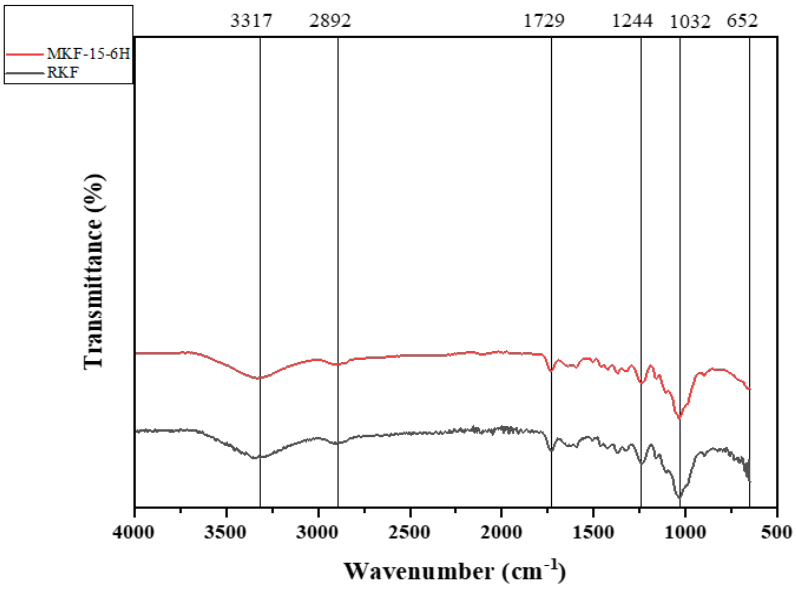

Fig. 3 *FTIR comparison between RKF and MKF-15-6H sample*

The peak at 1032 cm^{-1} represents C-C stretching vibrations. Research by Leonard and Martin [30], the wavenumber ranging from 1000 - 1162 cm^{-1} indicates the C-C stretching for kapok fiber. Another research by Aimee et al. [23], stated the peak at wavenumber 1032 cm^{-1} was due to C-O stretching vibration, representing the waxy cutin and cellulosic components of the kapok fibers. The peak intensity change at 652 cm^{-1} was observed for modified-ZnO kapok fiber samples compared to RKF as shown in Table 2. This may be due to the Zn-O bond on the fiber surface, as supported by Yuepeng et al. [32], where the study stated that the adsorption bands between 650 and 550 cm^{-1} were attributed to –O–Zn bonds. Another similar study also mentioned that the bonding between Zn–O is from 600 to 700 cm^{-1} [33].

Overall, the other peaks of MKF-15-6H sample did not show as significant changes as the O-H stretching peak, indicating that the presence of ZnO nanoparticles had the most noticeable effect on the hydroxyl groups within the kapok fiber. These alterations suggest that the total amount of –OH was reduced, and hydrophobic ZnO NPs were developed on the surface of the modified ZnO-kapok fiber [10].

Table 2 *Transmittance at specific wavenumber*

Sample	Peak wavenumber (cm^{-1})	Transmittance (%)
RKF	3317	73.14
	2892	85.29
	1729	78.98
	1244	69.12
	1032	38.52
	652	53.04
MKF-15-6H	3317	75.59
	2892	86.74
	1729	81.00
	1244	71.27
	1032	40.89
	652	66.14

3.2.2 Morphology Analysis using SEM

The morphology of raw and modified kapok fibers with ZnO NPs was characterized using a Scanning electron microscope (SEM). Fig. 4(a) below show the SEM images of raw kapok fiber while Fig. 4(b) represents modified-ZnO kapok fibers modification through a hydrothermal process with ZnO NPs. The raw kapok fibers (RKF) in Fig. 4(a) serve as the baseline, displaying silky and smooth surfaces due to a layer of wax on its surface [13]. As for the

modified-ZnO kapok sample, it can be observed that the coating of ZnO on kapok in Fig. 4(b) causes the surface to become rougher when compared to RKF. Surface roughness is one of the crucial factors that affect the oil sorption capacity of sorbent support by a study from Jintao et al. [34], suggests that coated kapok fibers have low surface energy and can significantly enhance their oil sorption capacity. This is attributed to the rough fiber surface, which plays a crucial role in oil retention. These fibers can absorb and retain oils such as gasoline, diesel, and soybean oil more effectively than raw fibers. Another study by Aimee et al. [23] also suggests that the coated kapok fibers increased surface roughness and improved hydrophobicity, enhancing the fiber's sorption capacities for various oils. The same study also mentioned that the coated fibers exhibited fast initial sorption and high removal efficiency for motor oil in water.

The incorporation mechanism of ZnO into the kapok fibers can be explained by considering the interaction between ZnO nanoparticles and the kapok fiber surface. During the modification process, kapok fibers were immersed in a ZnO nanoparticle solution. The hydroxyl groups on the surface of the kapok fibers facilitate the adsorption of ZnO nanoparticles through hydrogen bonding and Van der Waals forces. As the fibers are dried and cured, these interactions become stronger, resulting in a stable attachment of ZnO nanoparticles to the fiber surface. The granular appearance observed in the SEM images indicates that ZnO nanoparticles are not only adsorbed on the surface but also penetrate the porous structure of the kapok fibers. This penetration enhances the fiber's surface area and provides additional active sites for oil adsorption.

The SEM analysis confirms the successful incorporation of ZnO nanoparticles into the kapok fibers, as evidenced by the morphological changes observed in the SEM images. The roughened surface and granular deposits indicate that ZnO nanoparticles are effectively integrated into the fiber structure. This modification is expected to enhance the oil adsorption capacity of the kapok fibers due to the increased surface area and the introduction of additional active sites.

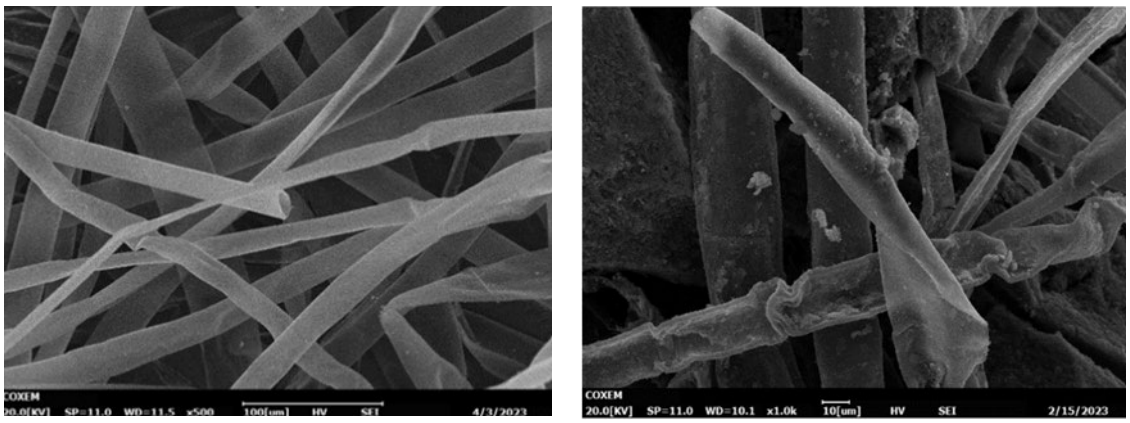

(a) **(b)**

Fig. 4 *(a) SEM images of raw kapok fiber (RKF); (b) SEM images of MKF-15-6H*

3.2.3 Wettability Analysis using Contact Angle

Fig. 5(b) shows that the water contact angle observed for sample MKF-15-6H, which is 142.20° and RKF contact angle was recorded at 125.5° as in Fig. 5(a). In contrast, Wang et al. [8], found that the contact angle of raw kapok fiber was 116°. However, the contact angle for raw kapok may differ depending on the country of origin [35]. As observed, the presence of ZnO coating on the kapok fiber surface, which will made fiber surface rougher compared to RKF. Bartolomeo et al. [36] explored how coating polypropylene fibers with nano-silica particles affected their surface roughness and revealed that coating volume could significantly impact the roughness of fiber surfaces.

Thus, surface roughness is among the factors influencing the contact angle and substrate wettability [37]. This comparison shows that modified kapok has a higher contact angle than the raw kapok, due to the differences in their surface roughness. Shima et al. [38] reported on developing superhydrophobic hollow cellulosic fibers for oil spill cleanup. The study found that the fibers' superhydrophobic characteristic, with a water contact angle of 140°, significantly contributed to their ability to absorb up to 100 g/g of oil, highlighting the direct relationship between hydrophobicity (high contact angle) and oil sorption capacity. Overall, these contact angle results are a crucial parameter that can be used to tailor the surface wettability properties of kapok fibers for specific applications, such as creating selective oil-absorbent materials that can be used for cleaning up oil spills while repelling water [39].

Int. Journal of Integrated Engineering Vol. 17 No. 8 (2025) p. 100-114

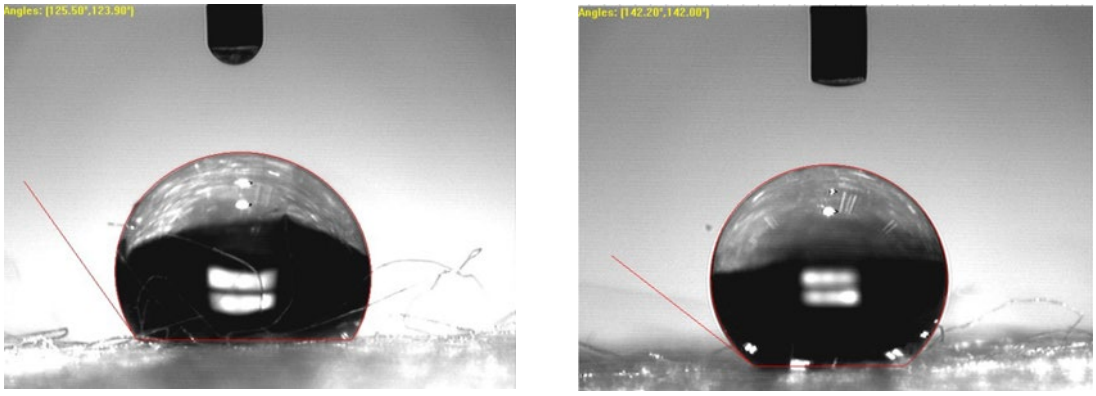

(a) **(b)**

Fig. 5 *(a) Water contact angle images of raw kapok fiber (RKF); (b) Water contact angle images of MKF-15-6H*

3.3 Kinetic Study of Kapok Fiber Oil Sorption

Over time, an oil sorption test was done using cooking oil as an oil medium to make the test more practical in real life. The test was done using RKF and MKF-15-6H samples, with an initial weight of 0.1 grams for both samples. All the procedures are as follows in Sub-chapter 2.3.4. Each sample was observed from 5 to 30 minutes, and the result was recorded as in Table 3 below.

Table 3 shows that both types of fibers start with zero oil sorption at time zero, which is expected as it marks the beginning of the observation period. In the first 5 minutes, both fibers showed a rapid increase in oil sorption, with RKF absorbing 77.6 g/g and MKF-15-6H absorbing slightly more at 78.7 g/g. This indicates that both fibers are initially very effective at oil adsorption. From 5 to 20 minutes, RKF steadily improves oil sorption, reaching 83.3 g/g. MKF-15-6H, on the other hand, shows a more variable trend, growing to 105.3 g/g at 10 minutes, then decreasing to 96.0 g/g at 15 minutes, and finally increasing to 97.3 g/g at 20 minutes. This indicates that MKF-15-6H has a larger but more variable adsorption capacity. At 25 and 30 minutes, both fibers demonstrate a rise in oil sorption, with RKF reaching 88.6 g/g and MKF-15-6H substantially higher at 114.7 g/g. RKF shows a gradual increase over this period, indicating that it has virtually reached equilibrium. However, MKF-15-6H has a larger total adsorption capacity, notably visible in the 25min to 30min time range.

MKF-15-6H consistently has a higher oil sorption capacity than RKF, demonstrating that the modification increases the fiber's ability to absorb oil. This could be owing to an increase in surface roughness [31], porosity [29], or chemical affinity [40] changes due to the modification process. The dynamics of oil sorption show that, while RKF absorbs oil at a consistent rate, MKF-15-6H has a variability, although not significant, notably in the 10 to 20-minute range. This could be attributed to the wavy surface of modified kapok fiber's, which is rougher than raw kapok, leading to a more intricate boundary condition between the oil and the fiber [41]. In summary, the modified kapok fiber (MKF-15-6H) has a higher oil sorption capacity than the raw kapok fiber (RKF), which is especially noticeable in the later phases of the observation period. This improved performance indicates that the modification procedure significantly improves the fiber's properties for oil spill remediation applications.

Table 3 *Adsorption data for both sample RKF and MKF-15-6H*

Time, t (min)	RKF (g/g)	MKF-15-6H (g/g)
0	0.0	0.0
5	77.6	78.7
10	77.0	105.3
15	78.0	96.0
20	83.3	97.3
25	88.0	103.7
30	88.6	114.7

3.3.1 Pseudo First Order Model

By fitting the oil sorption data over time into the Linear equation of the pseudo-order model, a graph plot of $\ln(q_e - q_t)$ vs time (t) was obtained. Fig. 6 shows the model fitting and parameter computations. Correlation coefficient (R^2) was used to determine the suitability of the linear fitted model for the system. The adsorption capacity at 30 minutes was chosen as the equilibrium value (q_e) for this model because kapok fiber usually achieved equilibrium

for the first 15 minutes [23]-[25]. Both the RKF and MKF-15-6H data have been fitted with a straight line. The slope of each line corresponds to the negative of the pseudo-first-order rate constant (k_1). The steeper slope for RKF indicates a higher rate constant and, thus, faster kinetics than MKF. The k_1 and q_e values were calculated by comparing Eq. (1) with the equation acquired from the predicted straight line.

The coefficient of determination (R^2) value of the model used to assess the goodness of fit of a regression model. An R^2 value of 1 indicates that the model perfectly predicts the data, while an R^2 value of 0 indicates that the model does not predict the data. The RKF has an R^2 of 0.819, which is high, indicating a good fit for the model. The MKF-15-6H, with an R^2 of 0.5859, suggests a poorer fit. Pseudo First order rate constant (k_1), for RKF and MKF-15-6H, were 0.1557 min^{-1} and 0.0755 min^{-1}, respectively.

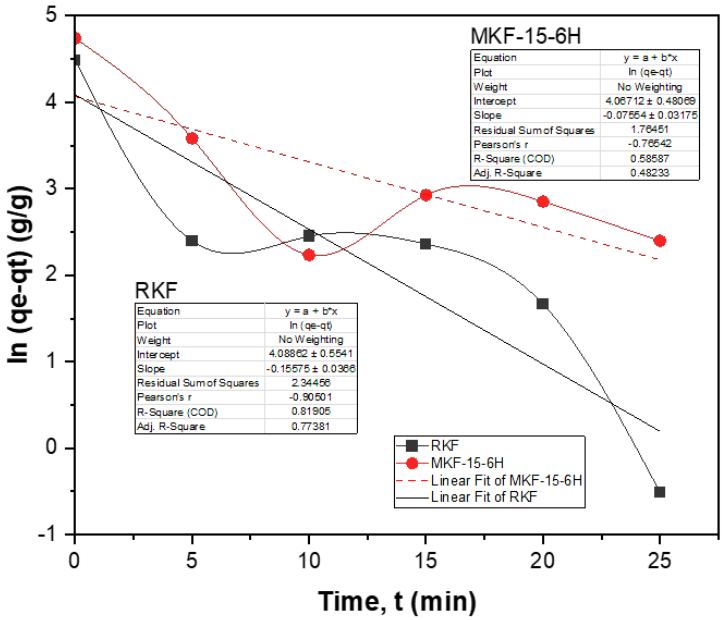

Fig. 6 *Linear pseudo first order fitted model*

3.3.2 Pseudo Second Order Model

A graph plot of t/q_t (g/g) vs. time, t (min), was obtained by fitting the oil sorption data over time into the Linear Pseudo Second Order model. Fig. 7 below shows the Linear Pseudo Second Order fitted model. Based on Fig. 7 above, the coefficient of determination (R^2) for RKF and MKF-15-6H were 0.9942 and 0.9781, respectively. This indicates that both RKF and MKF-15-6H show a great fit for the linear Pseudo second-order model with R^2 value above 0.9 compared to R^2 value for the Linear Pseudo First Order model. The Pseudo Second Order rate constant (k_2) for both RKF and MKF-15-6H was calculated from the linear equation y = mx + c of the predicted straight line according to the Eq. (5). By comparing the slope of the predicted straight line (m) with $1/q_e$, the q_e Predicted values for RKF and MKF-15-6H were 89.28 g/g and 111.11 g/g, respectively. Comparing the value of c of the predicted straight line with $1/ (k_2*q_e2)$, the k_2 value for both RKF and MKF-15-6H were 0.0107 g g^{-1} min^{-1} and 0.0076 g g^{-1} min^{-1} respectively.

Int. Journal of Integrated Engineering Vol. 17 No. 8 (2025) p. 100-114

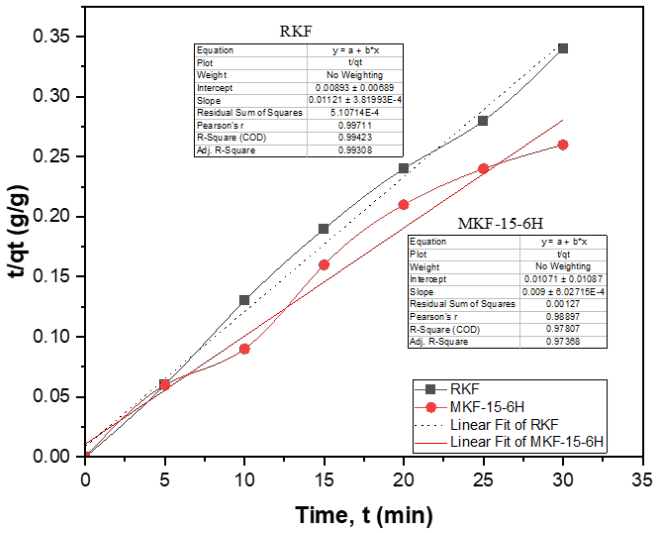

Fig. 7 *Linear pseudo second order fitted model*

3.3.3 Comparison of Kinetic Model

The Pseudo First Order (PFO) and Pseudo Second Order (PSO) model was compared by comparing the parameter as shown in Table 4. Based on the Table, Pseudo second Order kinetic model shows a great fit for this adsorption data with both RKF (0.9942) and MKF-15-6H (0.9781) coefficient of determination (R^2) value close to 1. As for the predicted value of q_e, the PSO predicted q_e value was closer to the original data than the predicted q_e value of PFO. Thus, suggests that both physical and chemisorption are present during oil sorption [31].

Using the sorption capacity values at specific time intervals (q_t) from Table 4, calculations were performed for both RKF and MKF-15-6H using Eq. (1) for PFO and Eq. (5) for PSO. Subsequently, the obtained data were used to plot a graph for the kinetic modelling of experimental data for RKF and MKF-15-6H, incorporating both PFO and PSO fittings, as depicted in Fig. 8. From Fig. 8, it is evident that the PSO-predicted data for sorption capacity at specific time intervals (q_t) closely match the experimental sorption capacity data for both RKF and MKF-15-6H, compared to the PFO-predicted data. Thus, PSO is more suitable for fitting an adsorption data of RKF and MKF-15-6H.

Table 4 *Adsorption data for both sample RKF and MKF-15-6H*

Kinetic model	Parameter	RKF	MKF-15-6H
Pseudo first order model	R^2	0.819	0.5859
	k_1	0.1557 min^{-1}	0.0755 min^{-1}
	q_e	59.65 g/g	58.39 g/g
Pseudo second order model	R^2	0.9942	0.9781
	k_2	0.0107 g g^{-1} min^{-1}	0.0076 g g^{-1} min^{-1}
	q_e	89.28 g/g	111.11 g/g

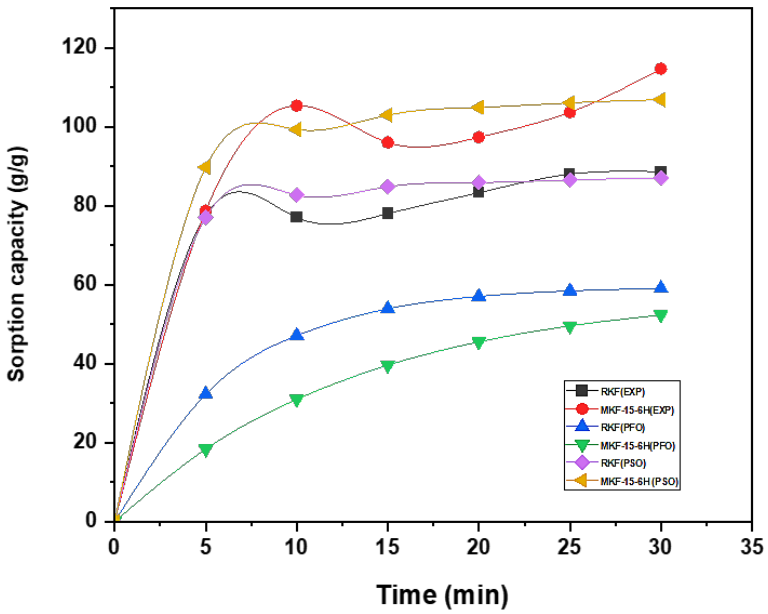

Fig. 8 *Kinetic modelling of experimental data for RKF and MKF-15-6H*

4. Conclusions

The modification of kapok fibers with ZnO nanoparticles through a hydrothermal process effectively enhances their oil adsorption capabilities. The kinetic study demonstrated that the pseudo second order model is better in representing the oil adsorption behaviour of both raw and modified kapok fibers, with modified-ZnO kapok showing a higher adsorption capacity compared to raw kapok. This suggests that both physical and chemical adsorption processes contribute to the overall adsorption mechanism. The findings of this study offer a promising approach for improving the efficiency of natural fiber-based oil sorbents, making them an environmentally friendly solution for oil spill remediation. Future studies should focus on optimizing the ZnO coating process to further enhance the adsorption efficiency and durability of the modified kapok fibers.

Acknowledgement

The authors would like to thank the Ministry of Higher Education (MOHE) for supporting this research under the Fundamental Research Grant Scheme (FRGS/1/2020/TK0/UTHM/02/45) and sponsored by Universiti Tun Hussein Onn Malaysia (UTHM) through Tier 1 (Vot Q916).

Conflict of Interest

Authors declare that there is no conflict of interest regarding the publication of the paper.

Author Contribution

The authors confirm contribution to the paper as follows: ***study conception and design:*** *M. A. Bukhori Hamidon, Rosniza Hussin;* ***data collection:*** *M. A. Bukhori Hamidon, Muhamad Zaini Yunos, Ainun Rahmahwati Ainuddin@Nordin;* ***analysis and interpretation of results:*** *M. A. Bukhori Hamidon, Rosniza Hussin, Zawati Harun;* ***draft manuscript preparation:*** *M. A. Bukhori Hamidon, Rosniza Hussin, Clement Pakiam, M. K. Azuan, U. S. Nabilah; All authors reviewed the results and approved the final version of the manuscript.*

References

[1] José Hidalgo-Crespo, César I. Alvarez-Mendoza, Manuel Soto & Jorge Luis Amaya-Rivas (2022) Towards a circular economy development for household used cooking oil in Guayaquil: Quantification, characterization, modeling, and geographical mapping, *Sustainability 14(15),* 1-14, 9565,

https://doi.org/10.3390/su14159565

[2] Dos Santos Ferreira, Luana, Aldara da Silva César, Marco Antonio Conejero & Ricardo César da Silva Guabiroba (2018) A voluntary delivery point in reverse supply chain for waste cooking oil: An action plan for participation of a public-school in the State of Rio de Janeiro, Brazil, *Recycling*, *3(4)*, 48,

https://doi.org/10.3390/recycling3040048

[3] A. Doraiah, Ray, Sibaprasad & Pankaj Gupta. (2007, March). *In-Situ Combustion Technique to Enhance Heavy-Oil Recovery at Mehsana, ONGC-A Success Story*. Paper presented at the SPE Middle East Oil and Gas Show and Conference, Manama, Bahrain. https://doi.org/10.2118/105248-MS

[4] Ankit Gupta & Rasna Gupta (2018) Treatment and recycling of wastewater from pulp and paper mill, In *Advances in Biological Treatment of Industrial Waste Water and Their Recycling for a Sustainable Future*, 13-49. Singapore: Springer Singapore. https://doi.org/10.1007/978-981-13-1468-1_2

[5] Qinglang Ma, Hongfei Cheng, Anthony G. Fane, Rong Wang & Hua Zhang (2016) Recent development of advanced materials with special wettability for selective oil/water separation, *Small*, *12(16)*, 2186-2202, https://doi.org/10.1002/smll.201503685

[6] Jian Li, Changcheng Xu, Changqing Guo, Haifeng Tian, Fei Zha & Lin Guo (2018) Underoil superhydrophilic desert sand layer for efficient gravity-directed water-in-oil emulsions separation with high flux, *Journal Of Materials Chemistry* A, 6(1), 223-230, https://doi.org/10.1039/C7TA08076J

[7] Yifei Long, Yongqian Shen, Haifeng Tian, Yaoxia Yang, Hua Feng & Jian Li (2018) Superwettable Coprinus comatus coated membranes used toward the controllable separation of emulsified oil/water mixtures, *Journal of Membrane Science*, 565, 85-94, https://doi.org/10.1016/j.memsci.2018.08.013

[8] Marat Nueraji, Zhexenbek Toktarbay, Aida Ardakkyzy, Deepak Sridhar, Hassan Algadi, Ben Bin Xu, Jalal T. Althakafy, Abdullah K. Alanazi, Hala M. Abo-Dief, Salimgerey Adilov, Zhanhu Guo (2023) Mechanically-robust electrospun nanocomposite fiber membranes for oil and water separation, *Journal of Environmental Research*, *220*, 115212, https://doi.org/10.1016/j.envres.2023.115212

[9] Zhong-Zheng Xu, Ming-Wei Zhao, Yi-Ning Wu, Jia-Wei Liu, Ning Sun, Zi-Zhao Wang, Yi-Ming Zhang, Lin Li & Cai-Li Dai (2023) Quantitatively probing interactions between membrane with adaptable wettability and oil phase in oil/water separation, *Journal of Petroleum Science*, 20(4), 2564-2574, https://doi.org/10.1016/j.petsci.2023.02.025

[10] Jintao Wang, Yian Zheng & Aiqin Wang (2012) Superhydrophobic kapok fiber oil-absorbent: Preparation and high oil absorbency. *Chemical Engineering Journal*, *213*, 1-7, https://doi.org/10.1016/j.cej.2012.09.116

[11] Apollo R. Agcaoili, Marvin U. Herrera, Cybelle M. Futalan & Mary Donnabelle L. Balela (2017) Fabrication of polyacrylonitrile-coated kapok hollow microtubes for adsorption of methyl orange and Cu (II) ions in aqueous solution. *Journal of the Taiwan Institute of Chemical Engineers*, *78*, 359-369, https://doi.org/10.1016/j.jtice.2017.06.038

[12] Shashwat S. Banerjee, Milind V. Joshi & Radha V. Jayaram (2006) Treatment of oil spill by sorption technique using fatty acid grafted sawdust. *Chemosphere*, *64(6)*, 1026-1031, https://doi.org/10.1016/j.chemosphere.2006.01.065

[13] Check Shyong Quek, Norzita Ngadi & Muhammad Abbas Ahmad Zaini (2020) The oil-absorbing properties of kapok fibre–a commentary, *Journal of Taibah University for Science*, *14(1)*, 507-512, https://doi.org/10.1080/16583655.2020.1747767

[14] Xiaofeng Huang & Teik-Thye Lim (2006) Performance and mechanism of a hydrophobic–oleophilic kapok filter for oil/water separation. *Desalination*, *190(1-3),* 295-307, https://doi.org/10.1016/j.desal.2005.09.009

[15] Koon Lau Tan, & B. H. Hameed (2017) Insight into the adsorption kinetics models for the removal of contaminants from aqueous solutions, *Journal of the Taiwan Institute of Chemical Engineers*, *74*, 25-48, https://doi.org/10.1016/j.jtice.2017.01.024

[16] Monday Musah, Yakubu Azeh, John Mathew, Musa Umar, Zulaihat Abdulhamid & Aishetu Muhammad (2022), Adsorption kinetics and isotherm models: A review, *Caliphate Journal of Science and Technology*, *4(1)*, 20-26, https://doi.org/10.4314/cajost.v4i1.3

[17] Emmanuel D. Revellame, Dhan Lord Fortela, Wayne Sharp, Rafael Hernandez & Mark E. Zappi (2020) Adsorption kinetic modeling using pseudo-first order and pseudo-second order rate laws: A review, *Cleaner Engineering and Technology*, *1*, 100032, https://doi.org/10.1016/j.clet.2020.100032

[18] Saeid Azizian (2004) Kinetic models of sorption: a theoretical analysis, *Journal of colloid and Interface Science*, *276(1)*, 47-52, https://doi.org/10.1016/j.jcis.2004.03.048

[19] Hamou Moussout, Hammou Ahlafi, Mustapha Aazza & Hamid Maghat (2018) Critical of linear and nonlinear equations of pseudo-first order and pseudo-second order kinetic models, *Karbala International Journal of Modern Science*, *4(2)*, 244-254, https://doi.org/10.1016/j.kijoms.2018.04.001

[20] M. E. L. Alouani, Saliha Alehyen, M. E. L. Achouri & M. Taibi (2018) Removal of cationic dye-methylene blue-from aqueous solution by adsorption on fly ash-based geopolymer, *Journal of Material and Environmental Science*, *9(1)*, 32-46, https://doi.org/10.26872/jmes.2018.9.1.5

[21] Jean-Pierre Simonin (2016) On the comparison of pseudo-first order and pseudo-second order rate laws in the modeling of adsorption kinetics, *Chemical Engineering Journal*, *300*, 254-263, https://doi.org/10.1016/j.cej.2016.04.079

[22] Yuh-Shan Ho & Gordon McKay (1999) Pseudo-second order model for sorption processes, *Process Biochemistry*, *34(5)*, 451-465, https://doi.org/10.1016/s0032-9592(98)00112-5

[23] Aimee Lorraine M. Blaquera, Marvin U. Herrera, Ronniel D. Manalo, Monet Concepcion Maguyon-Detras, Cybelle Concepcion M. Futalan & Mary Donnabelle L. Balela (2023) Oil adsorption kinetics of calcium stearate-coated kapok fibers, *Polymers*, *15(2)*, 452, https://doi.org/10.3390/polym15020452

[24] Jintao Wang, Yian Zheng & Aiqin Wang (2013) Preparation and properties of kapok fiber enhanced oil sorption resins by suspended emulsion polymerization, *Journal of Applied Polymer Science*, *127(3)*, 2184-2191, https://doi.org/10.1002/app.37783

[25] Baldin, Claudia Regina Bernardi, José Ilo Pereira Filho, and Vitor Baldin (2021) Estudo da influência da substituição do cimento Portland por resíduo de cerâmica vermelha na fabricação de placas de fibrocimento, *Matéria (Rio de Janeiro)*, *26*, e12914, https://doi.org/10.1590/s1517-707620210001.1219

[26] Murilo JP Macedo, Giovanna S. Silva, Michelle C. Feitor, Thércio HC Costa, Edson N. Ito & José DD Melo (2020) Surface modification of kapok fibers by cold plasma surface treatment, *Journal of Materials Research and Technology*, *9*(2), 2467-2476, https://doi.org/10.1016/j.jmrt.2019.12.077

[27] Graecia Lugito, Arip Kustiana, Reyhant Martuani & I. G. Wenten (2020) *Kapok fibre as potential oil-absorbing material: Modification mechanism and performance evaluation*. In IOP Conference Series: Materials Science and Engineering (Vol. 823, No. 1, p. 012033). IOP Publishing. https://doi.org/10.1088/1757-899x/823/1/012033

[28] Samsul Rizal Ikramullah, Sulaiman Thalib & Syifaul Huzni (2018, May) *Hemicellulose and lignin removal on typha fiber by alkali treatment*, In IOP Conference Series: Materials Science and Engineering (Vol. 352, p. 012019). IOP Publishing. https://doi.org/10.1088/1757-899X/352/1/012019

[29] G. Thilagavathi & C. Praba Karan (2019) Investigations on oil sorption capacity of nettle fibrous assembly and 100% nettle and nettle/kapok blended needle-punched nonwovens, *Journal of Industrial Textiles*, *49(4)*, 415-430, https://doi.org/10.1177/1528083718787532

[30] Leonard Y. Mwaikambo, & Martin P. Ansell (2002), Chemical modification of hemp, sisal, jute, and kapok fibers by alkalization, *Journal of Applied Polymer Science*, *84(12)*, 2222-2234, https://doi.org/10.1002/app.10460\

[31] Jintao Wang, Yian Zheng & Aiqin Wang (2012) Effect of kapok fiber treated with various solvents on oil absorbency, *Journal of Industrial crops and products*, *40*, 178-184, https://doi.org/10.1016/j.indcrop.2012.03.002

[32] Yuepeng Li, Degang Li, Wenyuan Han, Manqi Zhang, Bing Ai, Lipeng Zhang, Hongqi Sun & Zhen Cui (2019) Facile synthesis of di-mannitol adipate ester-based zinc metal alkoxide as a bi-functional additive for poly (vinyl chloride), *Polymers, 11(5)*, 813, https://doi.org/10.3390/polym11050813

[33] Zohra Nazir Kayani, Maryam Iqbal, Saira Riaz, Rehana Zia & Shahzad Naseem, (2015) Fabrication and properties of zinc oxide thin film prepared by sol-gel dip coating method, *Materials Science-Poland*, *33(3)*, 515-520, https://doi.org/10.1515/msp-2015-0085

[34] Jintao Wang, Yian Zheng & Aiqin Wang (2013) Coated kapok fiber for removal of spilled oil, *Journal of Marine pollution bulletin*, *69(1-2*) pp 91-96, https://doi.org/10.1016/j.marpolbul.2013.01.007

[35] Check Shyong Quek, Norzita Ngadi, and Muhammad Abbas Ahmad Zaini (2019) Kinetics and thermodynamics of dispersed oil sorption by kapok fiber, *Ecological Chemistry and Engineering*, *26(4)*, 759-772, https://doi.org/10.1515/eces-2019-0053

[36] Bartolomeo Coppola, Luciano Di Maio, Paola Scarfato & Loredana Incarnato (2015). Use of polypropylene fibers coated with nano-silica particles into a cementitious mortar, In *AIP Conference Proceedings*, 1695(1), 020056, AIP Publishing. https://.doi.org/10.1063/1.4937334

[37] Junchao Wang, Yankun Wu, Yijun Cao, Guosheng Li & Yinfei Liao (2020) Influence of surface roughness on contact angle hysteresis and spreading work, *Colloid and Polymer Science*, 298, 1107-1112, https://doi.org/10.1007/s00396-020-04680-x

[38] Shima Panahi, Meghdad Kamali Moghaddam & Meysam Moezzi. (2020) Assessment of milkweed floss as a natural hollow oleophilic fibrous sorbent for oil spill cleanup*, Journal of Environmental Management*, *268*, 110688, https://doi.org/10.1016/j.jenvman.2020.110688

[39] Gong Mao-Gang, Liu Yuan-Yue & Xu Xiao-Liang (2010) A new model for the formation of contact angle and contact angle hysteresis, *Chinese Physics B, 19(10)*, 106801,

https://doi.org/10.1088/1674-1056/19/10/106801

[40] Yongsoon Shin, Kee Sung Han, Bruce W. Arey & George T. Bonheyo (2020) Cotton fiber-based sorbents for treating crude oil spills, *ACS Omega*, 5(23), 13894-13901, https://doi.org/10.1021/acsomega.0c01290

[41] Yin Yao & Shaohua Chen (2013) The effects of fiber's surface roughness on the mechanical properties of fiber-reinforced polymer composites. *Journal of Composite Materials 47(23)*, 2909-2923, https://doi.org/10.1177/0021998312459871